Available online on 15.11.2026 at http://jddtonline.info

Journal of Drug Delivery and Therapeutics

Open Access to Pharmaceutical and Medical Research

Copyright © 2026 The Author(s): This is an open-access article distributed under the terms of the CC BY-NC 4.0 which permits unrestricted use, distribution, and reproduction in any medium for non-commercial use provided the original author and source are credited

Open Access Full Text Article

Research Article

Integrating qNMR, Spectroscopic Characterization, and In Silico Screening for Comprehensive Evaluation of Curcumin and Its Drug-Like Derivatives

Palak[1], Sneha[1], Parul Kumar[1], Ritika Gupta[1], Praveen Kumar[1], Inder Kumar*[1], Kapil Kumar Verma[2]

[1]Minerva College of Pharmacy, Indora, Kangra, HP, India

[2]Abhilashi College of Pharmacy, Nerchowk, Mandi, HP, India

Article Info:

Article History:

Received 18 Aug 2026
Reviewed 20 Sep 2026
Accepted 17 Oct 2026
Published 15 Nov 2026

Cite this article as:

Palak, Sneha, Kumar P, Gupta R, Kumar P, Kumar I, Verma KK, Integrating qNMR, Spectroscopic Characterization, and In Silico Screening for Comprehensive Evaluation of Curcumin and Its Drug-Like Derivatives, Journal of Drug Delivery and Therapeutics. 2026; 16(11):25-35 *DOI:* https://doi.org/10.22270/jddt.v16i11.8066

For Correspondence:

Inder Kumar, Minerva College of Pharmacy, Indora, Kangra, HP, India

Abstract

Curcumin is an important natural polyphenol, but its quality and composition can vary depending on the source, and its poor physicochemical properties limit its pharmaceutical development. This study aimed to compare the quality of curcumin obtained from homemade turmeric from Indora, Kangra, Himachal Pradesh, India, and a locally marketed turmeric sample, while also characterizing the extracts and evaluating newly designed curcumin derivatives using computational methods. The turmeric samples were extracted using ethanol-based Soxhlet extraction and analyzed by ^{1}H NMR, FTIR, and mass spectrometry. Curcumin-related signals were observed in both extracts, with stronger signals in the marketed turmeric sample. Since complete internal-standard and validation data were not available, the NMR comparison was considered semi-quantitative. Mass spectrometry confirmed a protonated molecular ion at *m/z* 369.3 with characteristic fragments near *m/z* 177 and 149, while FTIR confirmed the major functional groups of curcumin. Fourteen curcumin derivatives were further evaluated using SwissADME and other in silico tools. Compounds 2, 4, 9, and 12 showed the most favourable overall drug-likeness profiles, although compound 12 showed low predicted gastrointestinal absorption. Compounds 2–7 and 9–11 showed high predicted gastrointestinal absorption, and target prediction suggested possible interactions with kinases, proteases, membrane receptors, and other protein classes. Overall, the study demonstrates a simple integrated approach for turmeric quality assessment, curcumin characterization, and computational screening of curcumin derivatives. Compounds 2, 4, and 9 were identified as promising candidates for further experimental studies, while compound 12 requires structural optimization. Further synthesis, validated qNMR analysis, and biological studies are needed to confirm these findings.

Keywords: *Curcuma longa*, qNMR, FTIR, mass spectrometry, SwissADME, drug-likeness, BOILED-Egg, target prediction, natural-product drug discovery.

1. INTRODUCTION

Curcuma longa L. (Zingiberaceae) is a medicinal and culinary plant whose rhizome is a major source of curcuminoids. Curcumin, chemically described as diferuloylmethane, is the principal colored curcuminoid and has the molecular formula $C_{21}H_{20}O_6$ and a molecular mass of 368.38 g/mol.[1] Its structure comprises two substituted aromatic rings connected through a conjugated seven-carbon β-diketone-containing linker. The phenolic hydroxyl, methoxy, aromatic, and keto–enol functionalities contribute to its redox behavior, molecular recognition, and chemical reactivity. Curcumin has consequently been investigated across inflammatory, oxidative, microbial, proliferative, and other disease-related pathways.[2,3]

Despite extensive biological interest, curcumin remains a difficult pharmaceutical scaffold. It is poorly soluble in water, is susceptible to environmental and metabolic degradation, and shows limited systemic exposure after conventional oral administration. These limitations are accompanied by another practical challenge: turmeric and curcuminoid preparations are chemically variable. Genotype, geographical origin, agro-climatic conditions, maturity, post-harvest processing, extraction procedure, and commercial standardization can influence the relative abundance of curcumin, demethoxycurcumin, bisdemethoxycurcumin, and non-curcuminoid constituents. Therefore, analytical characterization is central not only to curcumin research but also to the quality assessment of turmeric-derived materials.[4,5]

Quantitative nuclear magnetic resonance (qNMR) has become an important approach for natural-product analysis because NMR signal area is intrinsically related to the number of contributing nuclei. When acquisition conditions permit complete relaxation and a suitable internal standard is used, analyte content can be calculated from signal integrals and stoichiometric relationships without a compound-specific external calibration curve. NMR also provides structural information through the chemical environments of resonating nuclei. However, the evidential strength of qNMR depends on reporting the internal standard, analyte and reference masses, selected non-overlapping

signals, proton numbers, relaxation delay, pulse conditions, integration strategy, and replicate analysis. Comparative spectral intensity alone should not be equated with validated quantitative purity.[5,6]

Orthogonal analytical techniques can strengthen the assignment of curcuminoids. FTIR spectroscopy identifies characteristic vibrational bands associated with phenolic hydroxyl groups, the conjugated β-diketone system, aromatic carbon–carbon bonds, and methoxy functionalities. Mass spectrometry complements these data by providing molecular-ion and fragmentation information. For curcumin, a protonated molecular species near m/z 369 and characteristic lower-mass aromatic fragments have been described. The combined interpretation of NMR, FTIR, and MS therefore provides a more defensible identity assessment than reliance on a single analytical signal.[7,8]

Curcumin is also a frequently explored medicinal-chemistry scaffold. Its two aromatic rings, phenolic and methoxy substituents, and central linker provide several positions for rational modification. Alteration of hydrophobic substitution, hydrogen-bonding capacity, linker length, saturation, and polar functionality can substantially change lipophilicity, topological polar surface area, flexibility, solubility, and predicted target recognition. Computational profiling is particularly useful at this stage because it can rapidly identify molecules with severe physicochemical liabilities before resource-intensive synthesis and biological testing.[9]

SwissADME integrates physicochemical descriptors, pharmacokinetic predictions, drug-likeness rules, medicinal-chemistry alerts, bioavailability radar visualization, and the BOILED-Egg model for passive gastrointestinal absorption and brain penetration. In parallel, ligand-based target-prediction approaches can generate hypotheses concerning likely protein families and potential polypharmacology. These predictions are prioritization tools rather than evidence of biological activity; their value lies in narrowing experimental hypotheses and identifying candidates for synthesis, assay development, docking, and mechanistic validation.[10,11]

Although curcumin extraction, analytical characterization, and computational derivative screening are widely studied, these stages are often reported independently. A sequential framework that begins with source-dependent material assessment, uses complementary analytical evidence to support curcuminoid identity, and then extends the confirmed scaffold into computational lead triage offers a coherent natural-product-to-lead discovery strategy. Accordingly, the present study integrated ethanol-based Soxhlet extraction of homemade and marketed turmeric preparations, comparative ^{1}H NMR/qNMR-oriented assessment, FTIR and mass spectrometric characterization, and in silico profiling of fourteen rationally designed curcumin derivatives. The objective was to establish an integrated workflow and identify derivatives with comparatively favorable drug-likeness and pharmacokinetic characteristics for subsequent experimental validation.[12,13]

2. MATERIALS AND METHODS

2.1 Study design

The investigation was organized as a sequential experimental–computational workflow. Turmeric samples from homemade and marketed sources were collected and extracted under comparable Soxhlet conditions. Extracted curcuminoid material was examined by ^{1}H NMR/qNMR-oriented spectral comparison. Structural evidence was complemented by FTIR spectroscopy and mass spectrometry. The curcumin scaffold was then used for structure–activity relationship-guided design of fourteen derivatives, which were evaluated computationally for physicochemical properties, pharmacokinetic behavior, medicinal-chemistry alerts, and putative target profiles.

2.2 Collection and preparation of turmeric samples

The homemade turmeric sample was obtained from Badukher, Indora, Kangra, Himachal Pradesh, India. Rhizomes were washed with clean water to remove adhering soil and visible impurities, air-dried at room temperature, and stored in a clean, dry container before powder preparation. The marketed turmeric powder was procured from the local market in Indora, Kangra, Himachal Pradesh, India, and stored in an airtight container at room temperature to minimize moisture uptake and degradation. Manufacturer, batch, manufacturing-date, and expiry details should be added to the final submission if available.

2.3 Soxhlet extraction of curcuminoids

For each sample, 5 g of turmeric powder was transferred to a Soxhlet thimble and extracted with 150 mL ethanol for 5–6 h under reflux. After extraction, the solution was allowed to cool and was filtered through Whatman No. 1 filter paper. Ethanol was removed by distillation to obtain a concentrated curcuminoid-rich extract. The same nominal extraction conditions were applied to homemade and marketed samples.[14,15]

2.4 Preparation of NMR samples

An accurately weighed amount of curcuminoid sample from the homemade and marketed preparations was dissolved in a known volume of DMSO-d6. The source report states that a precisely weighed internal standard was added and that solutions were transferred to clean, dry 5-mm NMR tubes. The identity and certified purity of the internal standard, exact analyte and standard masses, and final solution volumes were not retained in the consolidated source dataset and must be recovered from the original NMR worksheet before definitive qNMR concentration or purity values are reported.[16,17]

2.5 ^{1}H NMR and qNMR-oriented assessment

Proton NMR spectra were acquired at 600 MHz in DMSO-d6. Individual spectra for the curcumin-related sample, marketed preparation, and homemade preparation, together with a stacked spectral comparison, were examined for curcumin-associated signals and relative spectral response. In a fully validated qNMR procedure, analyte purity (Px) may be calculated relative to an internal standard according to

$$P_x = (I_x/I_{std}) \times (N_{std}/N_x) \times (M_x/M_{std}) \times (m_{std}/m_x) \times P_{std}$$

where I is integral area, N is the number of nuclei represented by the selected signal, M is molar mass, m is weighed mass, and Pstd is the purity of the standard. Because the necessary integral and acquisition metadata were unavailable, no numerical qNMR purity was reconstructed in the present integrated manuscript.[18]

2.6 FTIR spectroscopic characterization

FTIR spectroscopy was used to examine functional groups within the extracted curcuminoid material. Spectral interpretation focused on the broad phenolic O–H stretching region at approximately 3200–3500 cm−1, conjugated carbonyl/β-diketone-associated absorption near 1625–1650 cm−1, aromatic C=C bands around 1600 and 1500 cm−1, and C–O stretching bands in the 1260–1280 and 1020–1100 cm−1 regions associated with phenolic/methoxy functionality. Instrument model, sampling mode, resolution, and number of scans should be inserted from the original instrument record before submission.[7,9]

2.7 Mass spectrometric characterization

Mass spectrometric data were evaluated for curcuminoid molecular species and characteristic fragmentation. The source dataset reported protonated ions at m/z 369.3 for curcumin, 354.10 for demethoxycurcumin, and 342.7 for bisdemethoxycurcumin. Curcumin-related fragments near m/z 177 and 149 were interpreted as substituted aromatic fragments arising from cleavage of the conjugated linker and associated neutral losses. The final manuscript should specify the mass spectrometer, ion source, polarity, scan range, and source parameters from the raw analytical record.[8]

2.8 Rational design of curcumin derivatives

Fourteen curcumin derivatives (M1–M14) were designed using reported structure–activity relationship concepts. Modifications were directed toward changing aromatic substitution, hydrogen-bonding features, lipophilicity, polarity, and/or linker-related properties while retaining a curcumin-related pharmacophoric framework. The complete chemical structures and canonical SMILES used for computational analysis should be reproduced directly from the original molecular-design file.[5,10]

2.9 In silico physicochemical and ADME profiling

The designed structures were submitted as SMILES strings to SwissADME. The evaluated parameters included rotatable bonds, hydrogen-bond acceptors, topological polar surface area (TPSA), WLOGP, ESOL log S, predicted CYP3A4 inhibition, gastrointestinal (GI) absorption, pan-assay interference compound (PAINS) alerts, and Brenk structural alerts. Drug-likeness was interpreted using the multidimensional balance of size, polarity, lipophilicity, solubility, flexibility, and saturation rather than a single descriptor.[12]

2.10 Bioavailability radar and BOILED-Egg analysis

SwissADME bioavailability radar plots were examined across LIPO, SIZE, POLAR, INSOLU, FLEX, and INSATU dimensions. The BOILED-Egg model was used to visualize predicted passive GI absorption and blood–brain barrier (BBB) penetration in WLOGP–TPSA space. P-glycoprotein substrate status was interpreted according to the color coding of the model output.[11]

2.11 In silico target prediction

The designed molecules were subjected to ligand-based target prediction using the target-prediction function linked from the SwissADME workflow. Predicted targets were summarized by protein class and selected named targets were used to generate mechanistic hypotheses. Because target prediction is similarity based, predicted target classes and individual proteins were treated as putative and were not described as experimentally confirmed interactions.[19]

2.12 Candidate prioritization

Candidate prioritization integrated bioavailability-radar alignment, predicted GI absorption, WLOGP, TPSA, solubility, CYP3A4 inhibition, PAINS/Brenk alerts, and breadth/relevance of the predicted target profile. Compounds were ranked comparatively within the fourteen-molecule series. A compound was not classified as therapeutically active solely on the basis of target prediction.[12,11]

2.13 Statistical considerations

The available consolidated dataset did not contain replicate-level extraction or qNMR numerical measurements. Therefore, inferential statistical testing was not applied to the source-comparison results. Statements of statistical significance were avoided. Future validated qNMR experiments should be conducted in independent replicate preparations and reported as mean ± standard deviation with an appropriate between-group statistical test.

3. RESULTS

3.1 Curcuminoid extraction and sample appearance

Ethanol Soxhlet extraction of both turmeric preparations yielded concentrated yellow to orange curcuminoid-rich extracts. The common sample mass, solvent volume, and extraction time provided a comparable extraction framework. The available reports did not retain dried-extract weights; therefore, extraction yield percentages could not be compared quantitatively.[15]

3.2 Comparative ^{1}H NMR profiles of homemade and marketed preparations

The 600-MHz ^{1}H NMR dataset included spectra of the curcumin-related sample, the marketed preparation, the homemade preparation, and a stacked comparison. Curcumin-associated spectral features were evident in both source preparations. The marketed preparation displayed a greater overall curcumin-associated peak response than the homemade preparation. This observation is consistent with a difference in

curcuminoid abundance and/or sample composition. However, peak height alone is affected by concentration, acquisition, processing, line width, and normalization; consequently, the present integrated analysis interprets the observation as a semi-quantitative source difference rather than a validated purity determination.[20]

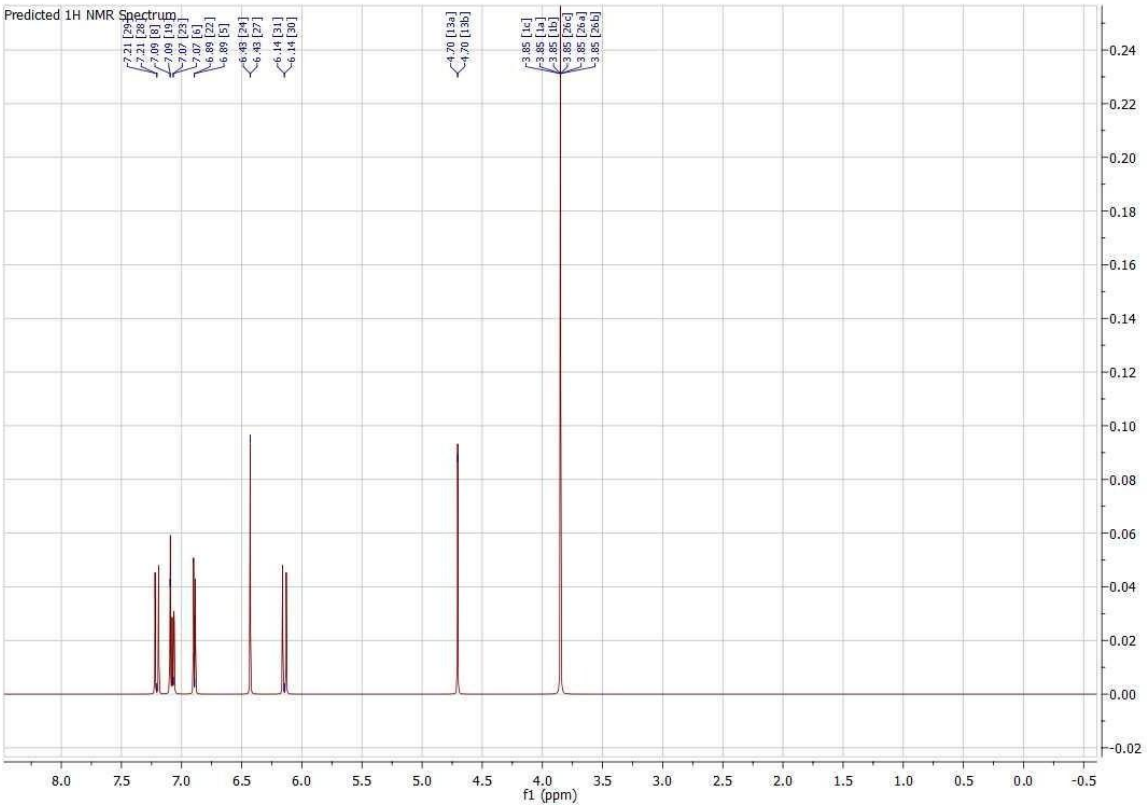


Figure 1A. ^{1}H NMR spectrum of the curcumin-related reference/sample.

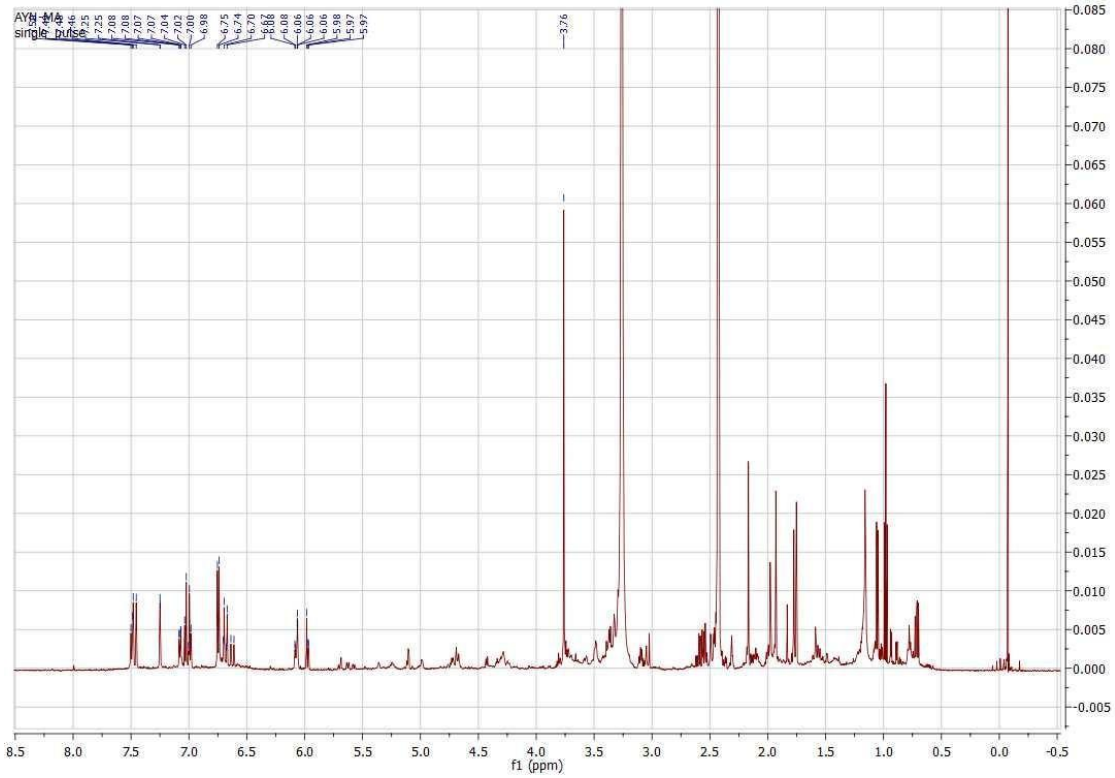


Figure 1B. ^{1}H NMR spectrum of the marketed curcumin preparation.

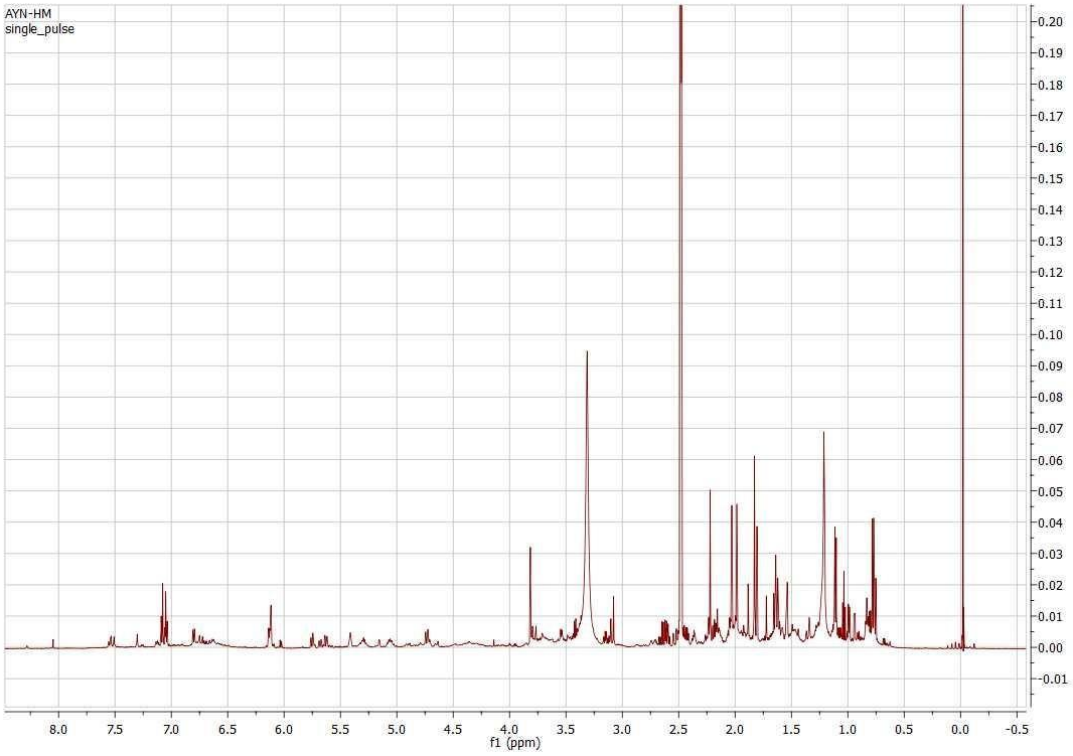


Figure 1C. ^{1}H NMR spectrum of the homemade *Curcuma longa*-derived preparation.

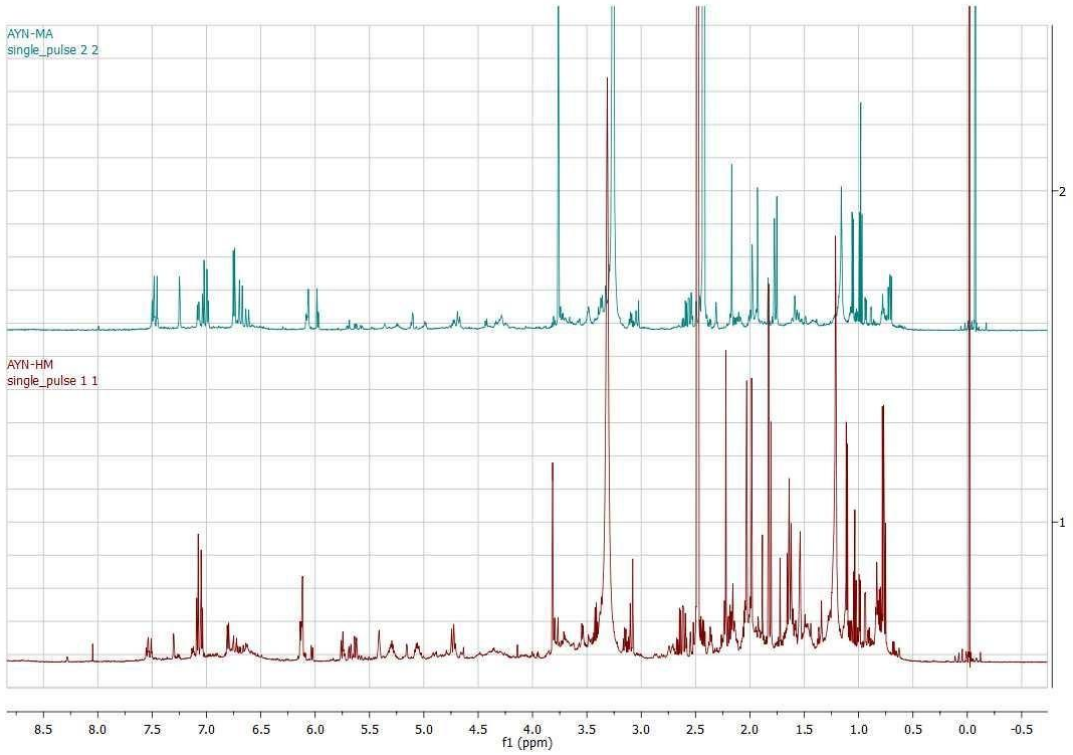


Figure 2. Stacked ^{1}H NMR spectra (600 MHz, DMSO-d_6) used for comparative assessment of marketed and homemade curcumin preparations.

3.3 qNMR reporting status

The experimental report described internal-standard-based qNMR preparation, but the consolidated records did not provide the internal standard identity, exact integral values, selected quantitative resonance, proton equivalence, relaxation delay, analyte and standard masses, or calculated concentrations. Accordingly, numerical curcumin concentration and purity values were not reconstructed. This conservative reporting prevents an unsupported quantitative claim and identifies the specific metadata required to upgrade the source comparison to a validated qNMR result.[16]

3.4 FTIR evidence for curcuminoid functional groups

FTIR analysis showed spectral regions consistent with the principal functionalities expected for curcuminoids. A broad band in the 3200–3500 cm−1 region was assigned to phenolic O–H stretching. Absorption near 1625–1650 cm−1 was consistent with the conjugated carbonyl/β-diketone system, whereas bands around 1600 and 1500 cm−1 supported aromatic C=C vibrations. C–O stretching features in the 1260–1280 and 1020–1100 cm−1 regions were compatible with phenolic and methoxy functionality. The overall pattern supported the presence of a curcumin-like conjugated polyphenolic structure.

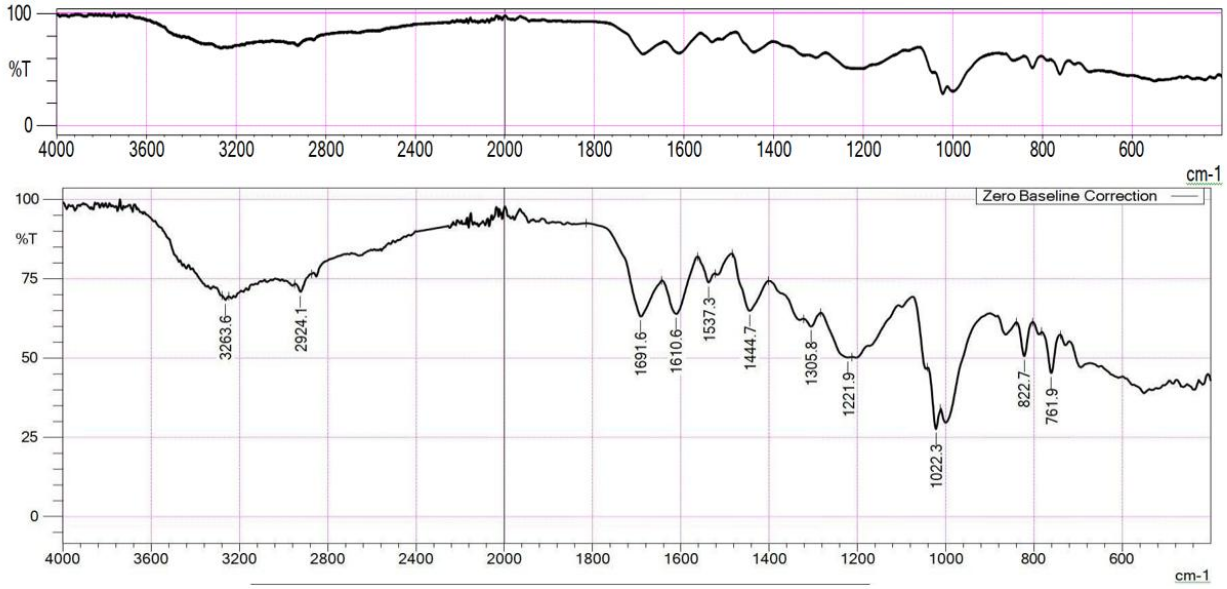


Figure 3. FTIR spectrum is embedded in the Results section.

3.5 Mass spectrometric evidence

Mass spectrometric analysis provided complementary molecular-mass and fragmentation evidence. A protonated curcumin-related molecular ion was reported at m/z 369.3. Demethoxycurcumin- and bisdemethoxycurcumin-related protonated ions were reported at m/z 354.10 and 342.7, respectively. For curcumin, prominent fragments near m/z 177 and 149 were associated with cleavage of the central conjugated chain and formation of stabilized substituted aromatic fragments. Together with the FTIR findings, the MS pattern supported curcuminoid identity.

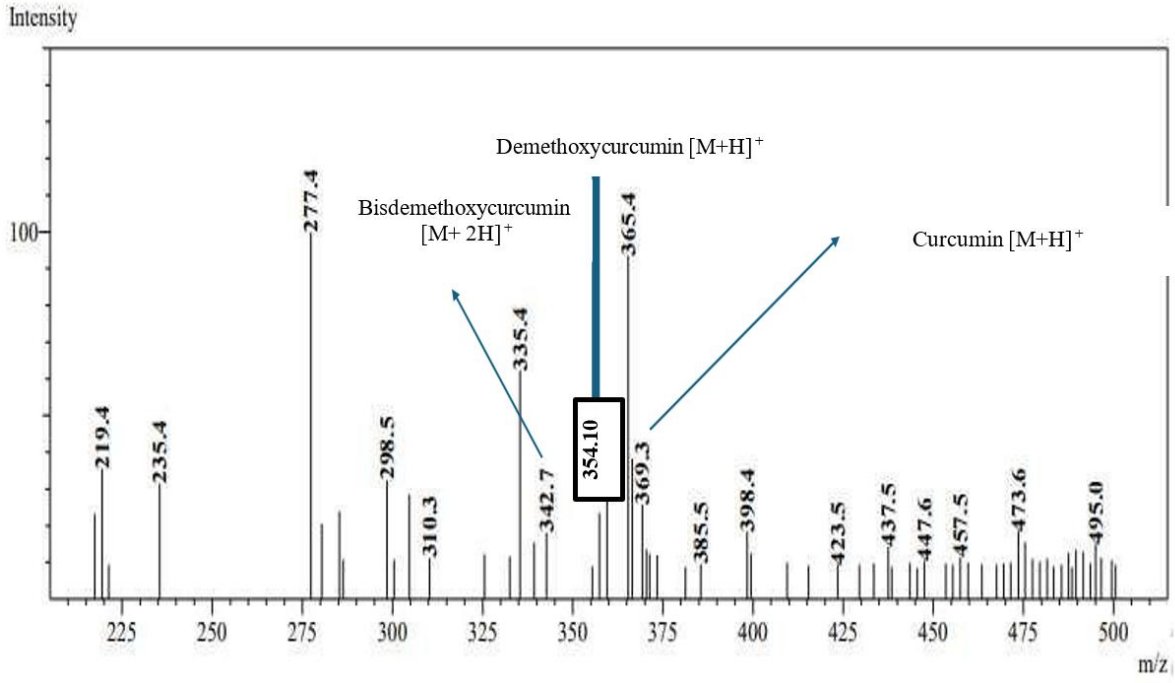


Figure 4. Mass spectrometric profile is embedded in the Results section.

3.6 Physicochemical and ADME profiles of the designed derivatives

The fourteen designed molecules displayed substantial physicochemical heterogeneity. Rotatable-bond counts ranged from 0 to 19, hydrogen-bond acceptors from 5 to 12, TPSA from 0 to 186.12 Å^2, and WLOGP from 2.25 to 10.23. Compounds M2–M7 and M9–M11 were predicted to have high GI absorption, whereas M1, M8, and M12–M14 showed low GI absorption. M7 had an exceptionally high WLOGP of 10.23, indicating a marked lipophilicity liability. M13 and M14 showed the least favorable ESOL log S values (−7.31). Predicted CYP3A4 inhibition was observed for M1, M2, M4, and M11. Most derivatives were free of PAINS alerts; M1, M13, and M14 carried alerts. Brenk alerts were present in several compounds.

3.7 Bioavailability radar and BOILED-Egg interpretation

Bioavailability-radar inspection indicated that M2, M4, M9, and M12 had comparatively better multidimensional alignment with the desirable physicochemical region than several other derivatives. M3, M5, and M13 showed more pronounced deviations associated with polarity, flexibility, and/or solubility-related characteristics. The BOILED-Egg plot placed the majority of derivatives in the region associated with probable passive gastrointestinal absorption, while few or none showed strong predicted BBB penetration. The distribution therefore favored peripheral exposure hypotheses over CNS-oriented development for most of the series. Several compounds were predicted P-glycoprotein substrates, indicating a possible efflux liability.

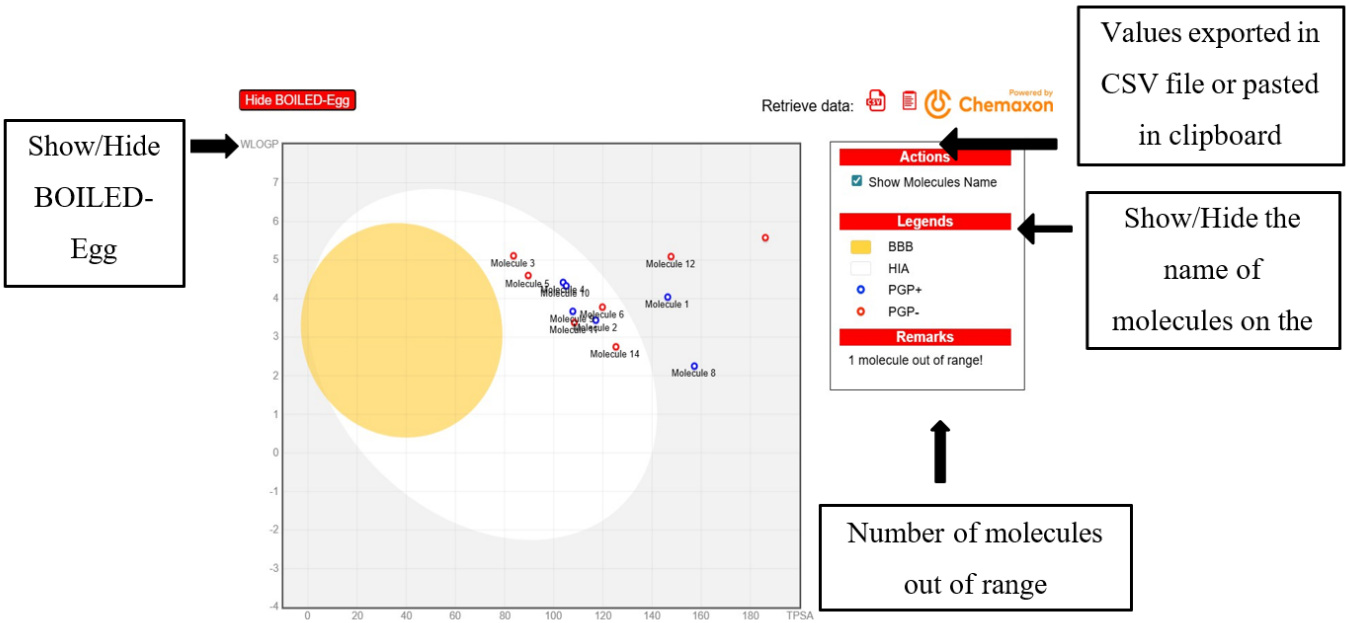


Figure 5. BOILED-Egg model for the fourteen designed curcumin derivatives showing predicted gastrointestinal absorption and blood–brain barrier disposition space.

3.8 Putative target-class profiles

Target prediction indicated marked polypharmacological diversity. Across the series, predicted classes included kinases, proteases, enzymes, phosphatases, membrane receptors, family A G protein-coupled receptors, transporters, ion channels, oxidoreductases, and epigenetic regulators. For M9, membrane receptors (26.7%) and proteases (20.0%) represented prominent predicted classes, with additional predictions including kinases (13.3%), adhesion molecules (13.3%), family A GPCRs (13.3%), oxidoreductases (6.7%), and enzymes (6.7%). Named putative targets included WEE1, mTOR, caspase-3, integrins, MMP12, SELL, SELP, LTB4R, and DHODH. These predictions suggest testable hypotheses involving cell-growth, apoptosis, adhesion, inflammatory signaling, and pyrimidine-metabolism pathways, but they do not demonstrate activity.

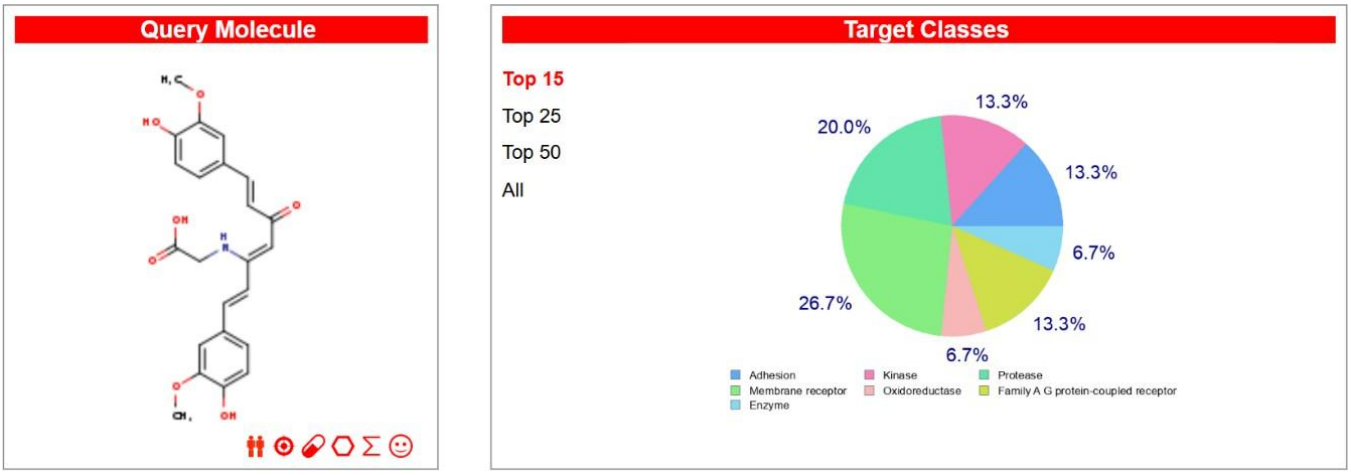


Figure 6. In silico target-prediction profile of Molecule 9 illustrating the distribution of predicted protein target classes.

3.9 Integrated candidate prioritization

M2, M4, M9, and M12 were initially highlighted by bioavailability-radar alignment. Integration with the tabulated ADME dataset refined this ranking. M2 combined high predicted GI absorption, WLOGP 3.44, TPSA 117.12 Å², no PAINS alert, and no Brenk alert, although predicted CYP3A4 inhibition requires attention. M4 showed high GI absorption and a favorable radar profile, but had two Brenk alerts and predicted CYP3A4 inhibition. M9 showed high GI absorption, WLOGP 3.67, TPSA 107.75 Å², no PAINS alert, and a broad target profile, although three Brenk alerts were present. M12 aligned comparatively well in the radar analysis but had low predicted GI absorption, 19 rotatable bonds, TPSA 147.72 Å², WLOGP 5.09, poor predicted solubility, and four Brenk alerts. Thus, M2, M4, and M9 were considered the most defensible immediate follow-up candidates, whereas M12 was retained as a secondary scaffold-optimization candidate.

Table 1. SwissADME-derived physicochemical, pharmacokinetic, and medicinal-chemistry parameters of M1–M14

Molecule	Rotatable bonds	HBA	TPSA (Å²)	WLOGP	ESOL log S	CYP3A4 inhibitor	GI absorption	PAINS	Brenk
1	8	5	146.38	4.04	-6.7	Yes	Low	3	3
2	9	6	117.12	3.44	-5.15	Yes	High	0	0
3	6	6	83.64	5.11	-5.56	No	High	0	0
4	11	9	103.82	4.42	-6.36	Yes	High	0	2
5	7	6	89.63	4.6	-5.78	No	High	0	0
6	7	6	119.83	3.78	-4.95	No	High	0	0
7	17	11	162.79	10.23	-4.95	No	High	0	0
8	14	10	157.24	2.25	-3.83	No	Low	0	3
9	13	10	107.75	3.67	-5.01	No	High	0	3
10	9	6	105.75	4.33	-5.01	No	High	0	3
11	12	8	108.36	3.38	-3.96	Yes	High	0	2
12	19	10	147.72	5.09	-6.39	No	Low	0	4
13	16	12	186.12	5.58	-7.31	No	Low	1	4
14	0	12	0	5.58	-7.31	No	Low	1	4

Table 2. Integrated prioritization of leading derivatives.

Candidate	Key strengths	Principal liabilities	Priority
M2	High GI absorption; WLOGP 3.44; TPSA 117.12 Å^2; no PAINS/Brenk alerts	Predicted CYP3A4 inhibition; poor predicted solubility	High
M4	High GI absorption; favorable radar alignment; WLOGP 4.42	CYP3A4 inhibition; 2 Brenk alerts; poor solubility	High
M9	High GI absorption; WLOGP 3.67; TPSA 107.75 Å^2; no PAINS alert; broad target hypotheses	3 Brenk alerts; poor predicted solubility	High
M12	Comparatively favorable radar geometry	Low GI absorption; 19 rotatable bonds; TPSA 147.72 Å^2; 4 Brenk alerts	Secondary optimization

4. DISCUSSION

The present work connects three stages that are commonly treated as separate research questions: source-related assessment of turmeric-derived curcuminoids, complementary analytical confirmation of the extracted scaffold, and computational prioritization of structurally modified derivatives. The central contribution is therefore methodological integration rather than a claim that computationally predicted derivatives have already demonstrated therapeutic efficacy.

The comparative NMR observations indicate that the marketed and homemade turmeric-derived samples were not spectrally equivalent. A greater curcumin-associated response was observed for the marketed preparation. Differences of this type are plausible because raw-material genotype, cultivation conditions, harvesting, storage, milling, and industrial processing can alter curcuminoid composition. Commercial processing may also employ blending or standardization practices that reduce batch heterogeneity. Conversely, locally prepared material may retain a broader range of matrix constituents. Nevertheless, the original report's inference that a higher peak height proves that the marketed sample is 'genuine' is not analytically justified. Authenticity requires validated identity and, where relevant, chemometric or marker-based comparison; peak height alone cannot establish genuineness.

A second important issue concerns the use of the term qNMR. True quantitative NMR requires traceable reporting of the quantitative signal, integral, internal standard, proton stoichiometry, weighing data, acquisition conditions, and relaxation behavior. The source report correctly described the principle of internal-standard qNMR and preparation in DMSO-d6, but the consolidated dataset did not preserve the numerical inputs needed to reproduce a purity calculation. Accordingly, this manuscript deliberately describes the current NMR comparison as qNMR-oriented and semi-quantitative. Recovering the original NMR worksheet could materially strengthen the article: a single table containing sample mass, internal-standard mass and purity, selected δ values, integrals, proton numbers, calculated curcumin concentration, purity, and replicate variability would convert the weakest part of the manuscript into a major analytical result.

The FTIR and MS data provide orthogonal structural support. The broad O–H region, conjugated carbonyl-associated band, aromatic C=C bands, and methoxy C–O regions collectively match the functional architecture expected for curcuminoids. Mass spectrometry further supported this assignment through the curcumin-related protonated ion at m/z 369.3 and characteristic lower-mass fragments around m/z 177 and 149. The reported ions corresponding to demethoxycurcumin and bisdemethoxycurcumin are also chemically consistent with a curcuminoid mixture. These techniques answer different analytical questions: FTIR supports functional-group composition, MS supports molecular mass and fragmentation, and NMR describes proton environments and can provide quantification when correctly validated. Their convergence is more informative than any single technique in isolation.

Having established curcumin as the central scaffold, the computational component examined whether rational structural modification could improve properties relevant to drug development. The fourteen derivatives covered a broad physicochemical space. This diversity is evident from the large ranges in flexibility, polarity, and lipophilicity. M7, for example, showed WLOGP 10.23, a value that strongly suggests excessive lipophilicity and raises concerns regarding aqueous solubility and nonspecific partitioning. At the opposite end of the property spectrum, highly polar compounds with TPSA values above approximately 140 Å^2 were more frequently associated with low predicted GI absorption. M13 combined high TPSA, high WLOGP, very poor predicted solubility, a PAINS alert, and four Brenk alerts, making it a weak lead-like candidate without substantial redesign.

The bioavailability radar initially highlighted M2, M4, M9, and M12. However, the integrated analysis demonstrates why visual radar alignment should not be used as a stand-alone ranking method. M12, despite comparatively favorable multidimensional radar overlap, had low predicted GI absorption, TPSA 147.72 Å^2, 19 rotatable bonds, WLOGP 5.09, ESOL log S −6.39, and four Brenk alerts. This discordance is scientifically informative: a visually acceptable balance across radar dimensions can coexist with specific liabilities that become evident only when individual descriptors and

pharmacokinetic predictions are examined. M12 should therefore be considered an optimization scaffold rather than an immediate lead.

M2 emerged as one of the most balanced molecules in the series. Its WLOGP of 3.44 and TPSA of 117.12 Å^2 were accompanied by high predicted GI absorption and absence of PAINS and Brenk alerts. The principal concerns were predicted CYP3A4 inhibition and poor predicted solubility. M4 similarly showed high GI absorption and favorable radar alignment, but CYP3A4 inhibition and two Brenk alerts reduce its attractiveness. M9 combined high GI absorption, moderate lipophilicity, TPSA 107.75 Å^2, and no PAINS alert. Although it carried three Brenk alerts, its broad predicted target profile generated several experimentally testable hypotheses. On the current evidence, M2, M4, and M9 form the most rational short list for synthesis and biological evaluation.

The BOILED-Egg results indicated that most designed derivatives were more compatible with predicted intestinal absorption than with BBB penetration. This is relevant to therapeutic positioning. The data do not support a general CNS-development claim for the series. Instead, peripheral indications are more consistent with the predicted disposition of most compounds. P-glycoprotein substrate predictions add another layer of complexity because efflux can limit cellular retention and tissue exposure. Future optimization should therefore consider permeability and transporter liability together rather than attempting to maximize lipophilicity alone.

Target-prediction outputs suggested polypharmacology across kinases, proteases, receptors, enzymes, and regulatory proteins. The M9 profile is illustrative: predicted classes included membrane receptors, proteases, kinases, adhesion molecules, GPCRs, oxidoreductases, and enzymes, with named hypotheses involving WEE1, mTOR, caspase-3, integrins, MMP12, SELL, SELP, LTB4R, and DHODH. Such a profile may be compatible with the broad biological literature surrounding curcumin-like scaffolds, but similarity-based prediction can also generate false positives and target promiscuity. Terms such as 'anticancer activity' or 'antimicrobial activity' should therefore not be assigned from these predictions alone. The appropriate interpretation is that the computational analysis identifies target hypotheses that can guide assay selection.

The integrated workflow has several strengths. First, it begins with real turmeric-derived material rather than an abstract scaffold. Second, it uses complementary analytical techniques to support curcuminoid identity. Third, it extends the experimentally relevant scaffold into a computational design space and applies multiple filters rather than selecting candidates on one descriptor. Finally, the workflow exposes data inconsistencies that would be obscured in separate project reports, such as the contrast between M12 radar alignment and its low GI absorption and high flexibility.

The study also has limitations. The botanical material was not linked to a reported voucher specimen or taxonomic authentication record. Marketed-sample batch metadata were incomplete. Extraction yield was not available. The qNMR dataset lacked the raw quantitative metadata required for reproducible purity calculation. FTIR and MS instrument parameters should be recovered from the original facility records. The designed derivatives were not synthesized, and no experimental solubility, permeability, metabolic, cytotoxicity, antimicrobial, or target-binding studies were conducted. Molecular docking and molecular-dynamics simulations were also not part of the present dataset. These limitations define a clear next stage rather than invalidating the workflow.

A rigorous follow-up study should first recover or repeat the qNMR experiment using a certified internal standard, a relaxation delay demonstrated to be adequate for the selected resonances, triplicate independent sample preparations, and a documented uncertainty assessment. In parallel, M2, M4, and M9 should be synthesized and structurally confirmed by NMR, high-resolution MS, and chromatographic purity analysis. Experimental aqueous/biorelevant solubility and permeability should precede broad biological claims. Target-specific assays can then be selected from the computational hypotheses. If antimicrobial development is intended, MIC and MBC testing against defined reference and clinically relevant strains should be performed, followed by target-focused biochemical assays. If oncology-oriented development is intended, cell-line selection should be driven by the predicted kinase/receptor profile and confirmed by pathway-level readouts. Docking and molecular dynamics may support these experiments but should not replace them.

5. CONCLUSION

This study presents an integrated experimental–computational workflow that links turmeric-source assessment, complementary curcuminoid characterization, and in silico optimization of the curcumin scaffold. Comparative 600-MHz ^{1}H NMR spectra indicated a greater curcumin-associated spectral response in the marketed preparation than in the homemade sample; however, the absence of complete internal-standard and integral metadata limited the current comparison to a semi-quantitative interpretation. FTIR bands corresponding to phenolic hydroxyl, conjugated carbonyl, aromatic, and methoxy functionalities, together with curcumin-related mass spectral ions and fragments, provided complementary evidence for curcuminoid identity. Computational evaluation of fourteen designed derivatives revealed marked differences in physicochemical and predicted pharmacokinetic behavior. Although M2, M4, M9, and M12 showed comparatively favorable bioavailability-radar profiles, integrated assessment identified M2, M4, and M9 as the most defensible immediate follow-up candidates, whereas M12 retained substantial absorption, flexibility, solubility, and structural-alert liabilities. The workflow provides a rational natural-product-to-lead prioritization framework, but validated

qNMR, synthesis of prioritized derivatives, experimental ADME characterization, and biological target validation are required before therapeutic efficacy can be claimed.

Ethics approval: Not applicable

Consent for publication: Not applicable.

Availability of data and materials: The analytical spectra, molecular structures, SMILES strings, and computational outputs should be deposited as supplementary material with the final journal submission.

Competing interests: The authors declare no competing interests.

Funding: None

Acknowledgements: The authors gratefully acknowledge the Minerva College of Pharmacy, Indora, Kangra, Himachal Pradesh, for academic and laboratory support.

REFERENCES

1. Hao M, Zhang C, Wang T, Hu H. Pharmacological effects, formulations, and clinical research progress of curcumin. Front Pharmacol [Internet]. 2025;Volume 16-2025. Available from: https://www.frontiersin.org/journals/pharmacology/articles/10.3389/fphar.2025.1509045 PMCid:PMC11955698 https://doi.org/10.3389/fphar.2025.1509045 PMid:40166470

2. Matthewman C, Krishnakumar IM, Swick AG. Review: bioavailability and efficacy of 'free' curcuminoids from curcumagalactomannoside (CGM) curcumin formulation. Nutr Res Rev [Internet]. 2023/01/19. 2024;37(1):14-31. https://doi.org/10.1017/S0954422423000033 https://www.cambridge.org/core/product/707713D95F40F825C182905D45595120 PMid:36655498

3. Cao HM, Zhao PH, Zhao YT, Fang JJ, Wang YN, Chen X. Recent Progress in Curcumin: Extraction, Purification, and Bioactivity [Internet]. Vol. 33, Current Medicinal Chemistry. 2026. p. 906-23. Available from: http://www.benthamscience.com/article/146130 https://doi.org/10.2174/0109298673353286241219061902 PMid:39865811

4. Kaur K, Al-Khazaleh AK, Bhuyan DJ, Li F, Li CG. A Review of Recent Curcumin Analogues and Their Antioxidant, Anti-Inflammatory, and Anticancer Activities. Vol. 13, Antioxidants. 2024. p. 1092. https://doi.org/10.3390/antiox13091092 PMid:39334750 PMCid:PMC11428508

5. Ahmed M, Basheer S, Mughram MHAL, Iqbal DN, Qamar S, Saeed A, et al. Structural development of curcumin: A natural product arsenal for diverse therapeutic targets- seizing opportunities through serendipity and rational design. J Mol Struct [Internet]. 2025;1324:140815. Available from: https://www.sciencedirect.com/science/article/pii/S0022286024033234 https://doi.org/10.1016/j.molstruc.2024.140815

6. Ocampos FMM, de Souza AJB, Ribeiro GH, Almeida LS, Cônsolo NRB, Colnago LA. NMR-based plant metabolomics protocols: a step-by-step guide. Front Nat Prod [Internet]. 2024;3-2024. Available from: https://www.frontiersin.org/journals/natural-products/articles/10.3389/fntpr.2024.1414506 https://doi.org/10.3389/fntpr.2024.1414506

7. Amsaraj R, Ranjan R, Rachaiah BP, Mutturi S. Multi-instrument spectroscopic study for authentication of curcumin content in commercial turmeric powders using machine learning algorithms. J Food Compos Anal [Internet]. 2024;134:106543. Available from: https://www.sciencedirect.com/science/article/pii/S0889157524005775 https://doi.org/10.1016/j.jfca.2024.106543

8. Guo S, Qiu S, Cai Y, Wang Z, Yang Q, Tang S, et al. Mass spectrometry-based metabolomics for discovering active ingredients and exploring action mechanism of herbal medicine. Front Chem [Internet]. 2023;Volume 11-2023. Available from: https://www.frontiersin.org/journals/chemistry/articles/10.3389/fchem.2023.1142287 https://doi.org/10.3389/fchem.2023.1142287 PMid:37065828 PMCid:PMC10102349

9. Kotha RR, Luthria DL. Curcumin: Biological, Pharmaceutical, Nutraceutical, and Analytical Aspects. Vol. 24, Molecules. 2019. p. 2930. https://doi.org/10.3390/molecules24162930 PMid:31412624 PMCid:PMC6720683

10. Afridi MB, Sardar H, Serdaroğlu G, Shah SWA, Alsharif KF, Khan H. SwissADME studies and Density Functional Theory (DFT) approaches of methyl substituted curcumin derivatives. Comput Biol Chem [Internet]. 2024;112:108153. Available from: https://www.sciencedirect.com/science/article/pii/S1476927124001415 https://doi.org/10.1016/j.compbiolchem.2024.108153 PMid:39067349

11. Daina A, Zoete V. A BOILED-Egg To Predict Gastrointestinal Absorption and Brain Penetration of Small Molecules. ChemMedChem [Internet]. 2016 Jun 6;11(11):1117-21. Available from: https://doi.org/10.1002/cmdc.201600182 https://doi.org/10.1002/cmdc.201600182 PMid:27218427

12. Daina A, Michielin O, Zoete V. SwissADME: a free web tool to evaluate pharmacokinetics, drug-likeness and medicinal chemistry friendliness of small molecules. Sci Rep [Internet]. 2017;7(1):42717. https://doi.org/10.1038/srep42717 PMid:28256516

13. Mullowney MW, Duncan KR, Elsayed SS, Garg N, van der Hooft JJJ, Martin NI, et al. Artificial intelligence for natural product drug discovery. Nat Rev Drug Discov [Internet]. 2023;22(11):895-916. Available from: https://doi.org/10.1038/s41573-023-00774-7 https://doi.org/10.1038/s41573-023-00774-7 PMid:37697042

14. Azmir J, Zaidul ISM, Rahman MM, Sharif KM, Mohamed A, Sahena F, et al. Techniques for extraction of bioactive compounds from plant materials: A review. J Food Eng [Internet]. 2013;117(4):426-36. https://doi.org/10.1016/j.jfoodeng.2013.01.014 https://www.sciencedirect.com/science/article/pii/S0260877413000277 PMCid:PMC9727548

15. Ashaolu TJ, Karaça AC, Rashidinejad A, Jafari SM. Recent advancements in curcumin extraction, chemical/bio-synthesis, purification, and food applications. Crit Rev Food Sci Nutr [Internet]. 2025 May 22;65(14):2714-30. Available from: https://doi.org/10.1080/10408398.2024.2349725 https://doi.org/10.1080/10408398.2024.2349725 PMid:38716814

16. Pauli GF, Jaki BU, Lankin DC. Quantitative 1H NMR: Development and Potential of a Method for Natural Products Analysis. J Nat Prod [Internet]. 2005 Jan 1;68(1):133-49. Available from: https://doi.org/10.1021/np0497301 https://doi.org/10.1021/np0497301 PMid:15679337

17. Ravaglia LM, de Oliveira PD, Holzgrabe U, Alcantara GB. qNMR in natural products: practical approaches. What nobody tells you before starting your qNMR study! Front Nat Prod [Internet]. 2024;3-2024. https://www.frontiersin.org/journals/natural-products/articles/10.3389/fntpr.2024.1416195 https://doi.org/10.3389/fntpr.2024.1416195

18. Malz F, Jancke H. Validation of quantitative NMR. J Pharm Biomed Anal. 2005;38(5):813-23. https://doi.org/10.1016/j.jpba.2005.01.043 https://www.sciencedirect.com/science/article/pii/S0731708505001597 PMid:15893442

19. Daina A, Michielin O, Zoete V. SwissTargetPrediction: updated data and new features for efficient prediction of protein targets of small molecules. Nucleic Acids Res. 2019 Jul 2;47(W1):W357-64. Available from: https://doi.org/10.1093/nar/gkz382 https://doi.org/10.1093/nar/gkz382 PMid:31106366

20. Gören AC, Çıkrıkçı S, Çergel M, Bilsel G. Rapid quantitation of curcumin in turmeric via NMR and LC-tandem mass spectrometry. Food Chem [Internet]. 2009;113(4):1239-42. Available from: https://www.sciencedirect.com/science/article/pii/S0308814608009783 https://doi.org/10.1016/j.foodchem.2008.08.014